Prior information improves tactile representation in primary somatosensory cortex

Pegah Kassraian[1,2]†, Finn Rabe[1], Marloes Maathuis[3], Nicole Wenderoth[1]

[1]Neural Control of Movement Lab, Department of Health Sciences and Technology, Swiss Federal Institute of Technology, Zurich, Switzerland

[2]Department of Neuroscience, The Kavli Institute for Brain Science, Mortimer B. Zuckerman Mind Brain Behavior Institute, Columbia University, New York, NY, USA

[3]Seminar for Statistics, Department of Mathematics, Swiss Federal Institute of Technology, Zurich, Switzerland

†Corresponding author: pegahkf@gmail.com

Successful navigation through the world requires the integration of sensory input with prior information about the environment. Although it has been shown that stimuli which match prior expectations can be detected faster and more accurately, little is known about the integration of prior information with incoming tactile stimulation in human somatosensory areas. It is also unknown if prior information can induce somatotopic activity in the primary somatosensory cortex (S1) in the absence of tactile stimuli. Based on a vibrotactile detection paradigm we assess how prior information impacts the behavioral performance of participants and how it concurrently modulates BOLD activity and multivariate representations of tactile stimuli in somatosensory areas within a human neuroimaging study. The supra-voxel somatotopic organization of S1 allows us to dissociate representations of tactile stimuli and the modulation thereof by prior information with the resolution permitted by fMRI. We find that vibrotactile stimuli that match participants' expectations enhance stimulus perception, and that this behavioral enhancement is associated with higher decoding accuracies of stimulus representations in the S1 and a concurrent decrease in BOLD levels in the area. Additionally, we show that prior cues are capable of inducing somatotopic BOLD activity even prior to the onset of tactile stimulation, that tactile stimuli can be decoded from this preparatory activity and that the precision of the decoding is related to the upcoming behavioral performance of participants.

Keywords. Prior information, Somatosensory cortex, Somatotopy, Tactile stimulation, Probabilistic processing, Decoding, Perception, MVPA, fMRI

Introduction

Humans can navigate their environment despite being continuously confronted with a wealth of unreliable sensory information. A central mechanism facilitating navigation is the integration of current sensory input with prior information on the environment. Studies of the visual system have underlined the role of prior

information in enhancing behavioral performance of participants, for instance in terms of reaction time or accuracy of visual stimulus detection [1, 2, 3]. Functional magnetic resonance imaging (fMRI) paradigms have concurrently found that behavioral improvements for sensory stimuli congruent with prior expectations are accompanied by a decrease in the blood oxygenation level dependent (BOLD) signal in early sensory areas [4, 2, 5, 6]. This observation is surprising, however, as traditionally an increase in BOLD levels has been associated with behavioral improvements. The use of decoding approaches, where for instance linear classifiers are used to predict the experimental condition based on the BOLD signal, has shed light on this surprising finding. For instance, it has been shown that the decrease in mean BOLD levels for visual stimuli congruent with participants' expectations was accompanied with higher decoding accuracies in early visual areas, and that the performance of the decoder was related to the behavioral performance of participants, thus suggesting an increase of signal to noise ratio for congruent stimuli [1,2].

Studies on the integration of prior information with sensory stimuli have traditionally focused on the visual domain and relatively little is known about the integration of prior information in the human somatosensory areas. It is for instance unknown how prior information modulates the BOLD activity in somatosensory areas and if such modulation takes place in early somatosensory areas or if prior information is integrated with incoming tactile information in higher order somatosensory processing regions. Moreover, although S1 has traditionally been considered as chiefly involved in the processing of afferent tactile stimuli, more recent studies have shown that the region can be activated even in the absence of incoming sensory stimulation, for instance during touch observation, tactile imagery or motor planning [25, 26, 49, 56]. Previous studies on visual and auditory stimuli have furthermore revealed that expectation increases baseline neural activity within category-specific regions in both early and late sensory areas even before stimulus onset [21, 23, 11, 12]. There is no consensus on the involvement of S1 in higher order processing of somatosensory information in the absence of tactile stimulation [52, 56]. It is unknown if probabilistic cues elicit somatotopic activity patterns in S1 in the absence of tactile input and how such activity would be associated with following behavioral detection performance. S1 provides a functional organization in the form of somatotopic maps which stretch over a range of voxels associated with the encoding of tactile stimulation of distinct digits, rendering those readily dissociable at the resolution permitted by fMRI and thus providing an optimal basis to assess these questions.

In this work, we study in particular how prior information on tactile stimuli modulates the BOLD activity in somatosensory cortices and how this modulation is associated both with behavioral performance of participants and with the ability to decode representations of individual fingers depending on probabilistic context. We further study if prior information induces changes in BOLD activity in somatosensory areas even before the onset of tactile information, if such BOLD activity is somatotopically organized, and how it is related to the following behavioral performance of participants.

To tackle these questions we designed a behavioral paradigm to assess the effects of expectation on perception and neural processing of somatosensory stimuli, based on behavioral and functional magnetic resonance imaging (fMRI) and the combination of univariate and multivariate analysis methods. The impact of expectation was explored within a vibrotactile discrimination paradigm where participants had to discriminate between weak, near-threshold stimulation of either their ring finger or thumb. The intensities of the vibrotactile stimulation were set around the participants' detection thresholds, so that perceptual uncertainty should reinforce the use of probabilistic prior information [15].

We found that finger representations from vibrotactile stimulations consistent with participants' prior expectations were associated with higher BOLD information content as quantified by linear decoding accuracy, that this information revealed a strong association with behavioral performance of participants,

and that it was aligned with the somatotopic organization of the contralateral S1 area. In addition, we found that probabilistic cues induced anticipatory activity patterns in the contralateral S1 hand area in the absence of tactile stimulation, that these patterns were informative in that they allow for the decoding of cued fingers, and that they exhibit similarities to the BOLD activity patterns associated with vibrotactile stimulation. Contrary to a recent human MEG study [12], where expectation induced category-specific anticipatory activity but not a suppression of the neuronal signal could be observed, our results showed attenuation of the BOLD signal during expected stimulation events, and this attenuation revealed somatotopic organization. Surprisingly, none of our findings extended to higher order somatotopic regions such as the secondary somatosensory area.

Results

Vibrotactile task paradigm

The experimental design is visualized in Fig 1. Twenty-five participants (both male and female) took part in a total of eight imaging runs where we assessed the impact of prior information on their vibrotactile discrimination performance over the course of two days (40 vibrotactile discrimination trials per run; Fig. 1A; Materials and Methods). Prior to each imaging run, the vibrotactile detection thresholds of each participant's ring finger and thumb were determined with an interleaved one-up one-down staircase (Fig. 1B; Materials and Methods).

Each trial consisted of three parts (Fig. 1C). First, visual prior information was shown, as described in the next paragraph. Second, there was vibrotactile stimulation of either the ring finger or the thumb of the participant's left hand. Stimulation intensities were sampled from a skew-normal distribution with the mode set to the participant's detection threshold of the respective finger. The use of weak vibrotactile stimulation of near-detection threshold intensity was meant to reinforce the use of prior information for the detection task. Third, there was a response period in which participants had to choose one of the three response options: 'Thumb', 'Ring finger' or 'None' if no stimulation was perceived (Fig 1C). The arrangement of the three response options on the screen was randomized between the different trials to preclude preparatory motor movements. The three parts of the trial were separated by intervals of variable lengths, during which subjects were instructed to focus on a fixation cross.

Prior information was provided to participants in the form of a square displayed on different parts of the screen: left, center, or right side of the screen). Subjects were informed that a square on the left indicated that vibrotactile stimulation of the ring finger was to follow with 80% probability (ring finger cue), that a square on the right indicated that stimulation of the thumb was to follow with 80% probability (thumb cue), and that a square in the middle indicated that stimulation of ring finger or thumb was equally likely (uninformative cue). The ring finger and thumb were chosen because of their anatomically distinct representation in S1 [16, 50]. The visual cue location was spatially consistent with the position of the cued finger of participant's left hand, thus ensuring an intuitive mapping for the participants. We refer to the trials where the stimulated finger was in line with the finger cue as belonging to the 'congruent' experimental condition (ring finger cue - stimulation of ring finger; thumb cue - stimulation of thumb), and to the trials where the stimulated finger was contrary to the participant's expectation as belonging to the 'incongruent' experimental condition (ring finger cue - stimulation of thumb; thumb cue - stimulation of ring finger). Trials with the uninformative cue belong to the 'uninformative' experimental condition.

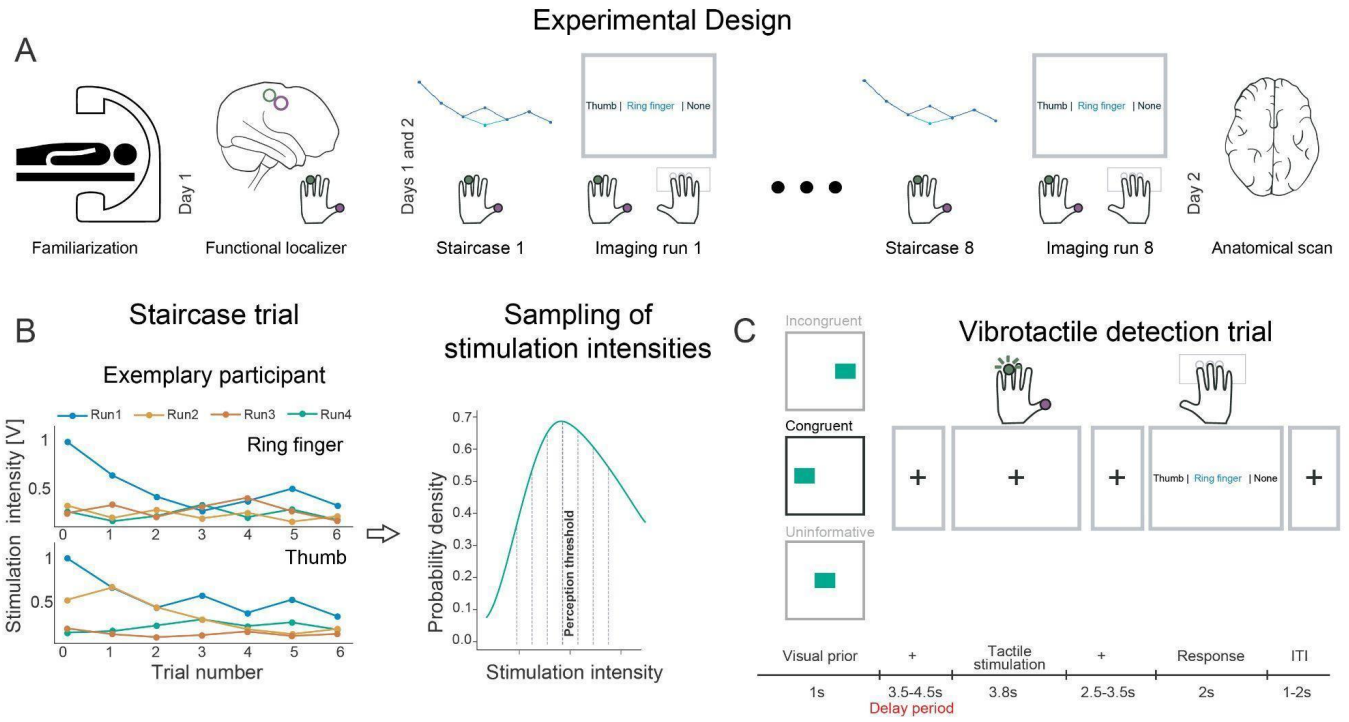

Figure 1 | Experimental design. (**A**) 25 Participants took part in a perceptual discrimination task where vibrotactile stimulation was applied to either ring finger or thumb of their left hand during concurrent fMRI data acquisition. Familiarization with the experimental environment was followed by four imaging runs per day on two subsequent days. Imaging runs on day one were preceded by the acquisition of functional localizers and imaging runs on day two were followed by the acquisition of structural MRI scans. Participants finished 40 vibrotactile detection trials per imaging run, totaling in 320 trials for the 8 runs. **(B)** The vibrotactile detection thresholds of each participant's ring finger and thumb were determined with an interleaved one-up one-down staircase prior to each imaging run. Vibrotactile stimulation intensities were sampled around this detection threshold for the following imaging run (see Materials and Methods). **(C)** Each trial started with the display of a probabilistic finger cue in the form of a square on different parts of the screen: ring finger cue (square on the left), thumb cue (square on the right), or uninformative cue (square in the middle). This was followed by vibrotactile stimulation of either ring finger (80% likely after ring finger cue; 50% likely after uninformative cue) or thumb (80% likely after thumb cue; 50% likely after uninformative cue) of the participant's left hand. During a subsequent response period participants could indicate where they had perceived the stimulation ('Thumb', 'Ring finger,' or 'None' if no stimulation was detected). Participants used their right hand for key presses on a button box to choose a response. The order of response options on the screen was randomized between trials. Trials were classified as belonging to the 'congruent' experimental condition (thumb cue - stimulation of thumb; ring finger cue - stimulation of ring finger), 'incongruent' experimental condition (thumb cue - stimulation of ring finger; ring finger cue - stimulation of thumb), or 'uninformative' experimental condition (uninformative cue). The three parts of each trial were separated by intervals of variable lengths where participants were instructed to focus on the fixation cross. Trials were separated by an inter-trial interval (ITI) of variable lengths (uniform sampling of 1-2s). Shown is an exemplary congruent trial with a ring finger cue (black square; gray squares show possible alternatives) and ring finger stimulation.

Prior information enhances vibrotactile detection performance

Previous literature has shown that prior information about sensory stimuli can facilitate perceptual performance, for instance in terms of detection accuracy [2,3]. In line with these findings we hypothesized that detection accuracies would be highest in the congruent experimental condition. This was indeed the case: detection accuracies were highest for the congruent condition, followed by the uninformative and then the incongruent condition (Fig. 2A). The differences between the behavioral detection accuracies of the three different experimental conditions were reflected in the psychophysical curves where a left shift for the congruent condition was indicative of an increase in detection accuracy as compared to the other two experimental conditions (Suppl. Fig. 1). Stimulation intensities did not differ significantly between the experimental conditions (Materials and Methods and Suppl. Table 1). This ensured that differences in

behavioral performance and BOLD activity levels were caused by differences in the prior information and not by the intensities of the vibrotactile stimulation.

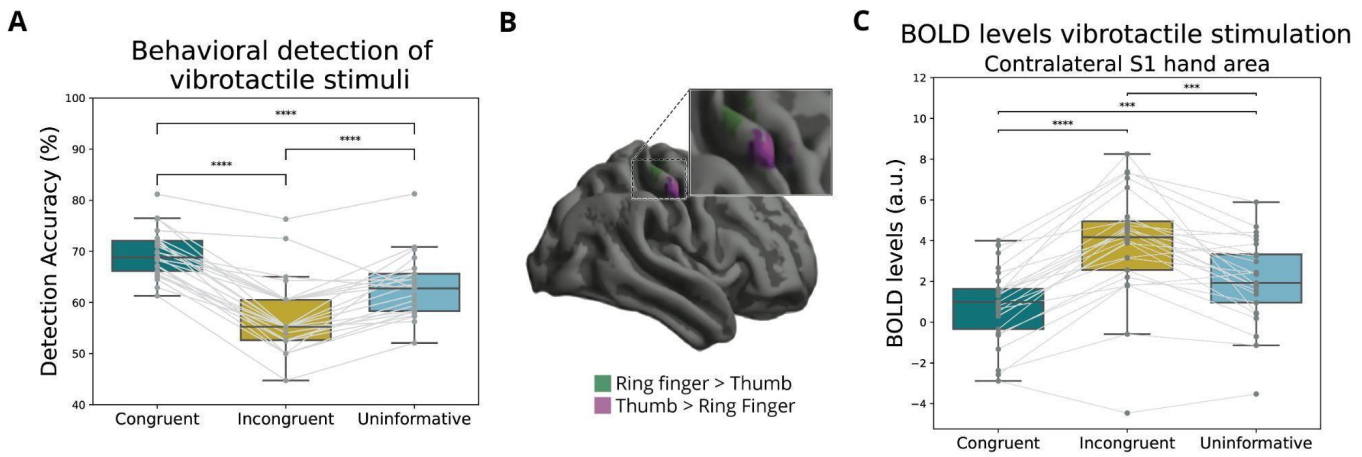

Figure 2. Influence of prior information on tactile detection performance. (**A**) Boxplots of behavioral detection accuracies of vibrotactile stimulation to ring finger or thumb for N=25 participants for the three different experimental conditions: congruent (70±4.8%), incongruent (61±6.8%) and uninformative (56±6%; all values mean±SEM). Single-participant-results are visualized by gray lines. The detection accuracy was significantly different among the three experimental conditions in a one-way repeated measures ANOVA ($F_{2,48}$ = 87.839, $p < 0.001$, $\eta^2 = 0.416$), and also in pairwise t-tests with post-hoc Bonferroni correction (significance indicated by stars: *** $p < 0.001$, **** $p < 0.0001$). (**B**) Contralateral S1 regions with increased activation during stimulation of a ring finger (green) or thumb (purple). Contrasting vibrotactile stimulation of ring finger and thumb confirmed separate clusters in areas 3b and 1 in the contralateral S1 hand area with a peak t-value of 5.18 for ring finger > thumb (MNI coordinate 42, -24, 60; cluster of 73 voxels total) and a peak t-value of 8.45 for thumb > ring finger (MNI coordinate 54, -14, 50; cluster of 128 voxels total; both results $p<0.05$, familywise error (FWE) corrected). Activation maps are from a second level GLM over all participants based on first-level analysis where vibrotactile stimulation of ring finger and thumb were contrasted to resting baseline with separate regressors for each finger and separate intercepts for each run and each participant. (**C**) Boxplots of average BOLD activity levels for the contralateral S1 hand area during vibrotactile stimulation: congruent (0.796±0.368), incongruent (3.887±0.539) and uninformative (2.029±0.415). Single-participant-results are visualized by gray lines. The average BOLD activity level was significantly different among the three experimental conditions in a one way repeated-measures ANOVA ($F_{2,48}$ = 44.466, $p < 0.001$, $\eta^2 = 0.252$), and also in pairwise t-tests with post-hoc Bonferroni correction (significance indicated by stars, as in Fig 2A).

BOLD levels of congruent stimuli are suppressed within the S1 hand area

We performed a univariate contrast of ring finger and thumb stimulation with a general linear model (GLM; Materials and Methods) to assess clusters of significant BOLD activity associated with vibrotactile stimulation of each finger. The contrast revealed two distinct clusters of voxels, one coinciding with the somatosensory ring finger region and one with the somatosensory thumb region, in agreement with an independent localizer task where supra-threshold stimuli were applied (Fig. 2B, Materials and Methods) and in line with previous studies investigating finger somatotopy [18]. Next, we extracted beta estimates from the GLM to compare the magnitude of BOLD responses of vibrotactile stimulation events within the contralateral S1 hand area between the three different experimental conditions (Materials and Methods). Previous studies have found a decrease in the BOLD signal when sensory stimuli were congruent with participants' expectations as compared to BOLD levels of 'incongruent' sensory stimuli [2, 20]. Our results confirmed these findings in that the average BOLD level within the contralateral S1 hand area was significantly lower in the congruent experimental condition when compared to the incongruent and uninformative experimental conditions (Fig. 2C).

Congruent stimuli can be decoded with highest accuracies

Previous studies have shown that BOLD activity patterns of visual stimuli congruent with participants' expectations are associated with higher decoding accuracies, suggesting a higher multivariate information content despite the univariate decrease of average BOLD level associated with this condition [4, 2, 6]. Vibrotactile stimuli are particularly well suited to assess this finding as different fingers are represented with supra-voxel in the somatosensory cortices, thus allowing an assessment of the effect of prior information on distinct somatotopic representations.

We used a linear classifier to decode stimulated finger (ring finger or thumb) based on BOLD activity level and investigated how decoding accuracies, and hence the information contained in the BOLD activity, differed between the three experimental conditions during vibrotactile stimulation. We found that decoding accuracies were only significantly above chance level for the congruent and the uninformative conditions and only in the contralateral S1 hand area (Fig. 3A). In addition, decoding accuracies were significantly higher in the congruent than in the uninformative or the incongruent conditions. Decoding accuracies were not significantly different from chance level in secondary somatosensory cortices, in the primary motor cortex and in further control regions. These results confirmed the surprising finding that the BOLD signal associated with congruent vibrotactile stimulation contained the highest amount of information to dissociate between the stimulated fingers.

Next, we employed a searchlight decoding approach where a linear classifier was applied to each voxel of the imaging data and each of its surrounding voxels (searchlight radius = 1). This allowed us to obtain finer localizations of decoding accuracies and to explore tactile representations throughout the brain. Group-level results revealed clusters of voxels associated with significant decoding accuracy against chance only for the congruent condition (one-sided t-test against chance level; FWE-corrected; Fig. 3B) with the largest cluster being located in the contralateral SI and primary motor cortex areas (787 voxels total; 62.6±4.3% decoding accuracy, mean±SEM across participants). Significantly higher decoding accuracies between congruent and incongruent and congruent and uninformative conditions were associated with clusters in the contralateral S1 hand area, located close to the thumb and ring finger peak voxels as determined by the univariate GLM analysis (Fig. 3B, Suppl. Table 2).

Although the somatotopic representation of fingers in S1 is well-established, it is not known whether the precision of the encoding of vibrotactile stimuli in the contralateral S1 area is related to the behavioral ability to discriminate between vibrotactile stimuli. To answer this, we compared the behavioral discrimination accuracy for vibrotactile stimulation of ring finger vs. thumb with the accuracy of S1 hand area-based decoding. In particular, we calculated the differences of behavioral detection accuracies between congruent and uninformative conditions and compared those to the difference in decoding accuracy between congruent and uninformative conditions (Fig. 3C). This comparison revealed a strong correlation between behavioral and BOLD decoding in the contralateral S1 hand area, suggesting the behavioral relevance of the decoding accuracy. In contrast, there was no correlation between improvements of behavioral performance and decoding accuracy within the ipsilateral S1 hand area or the regions extracted by a white matter mask used as a control.

Taken together, these results underline that finger representations from vibrotactile stimulations consistent with participants' prior expectations are associated with higher BOLD information content, that this information reveals a strong association with behavioral performance and that it is aligned with the somatotopic organization of the contralateral S1 area.

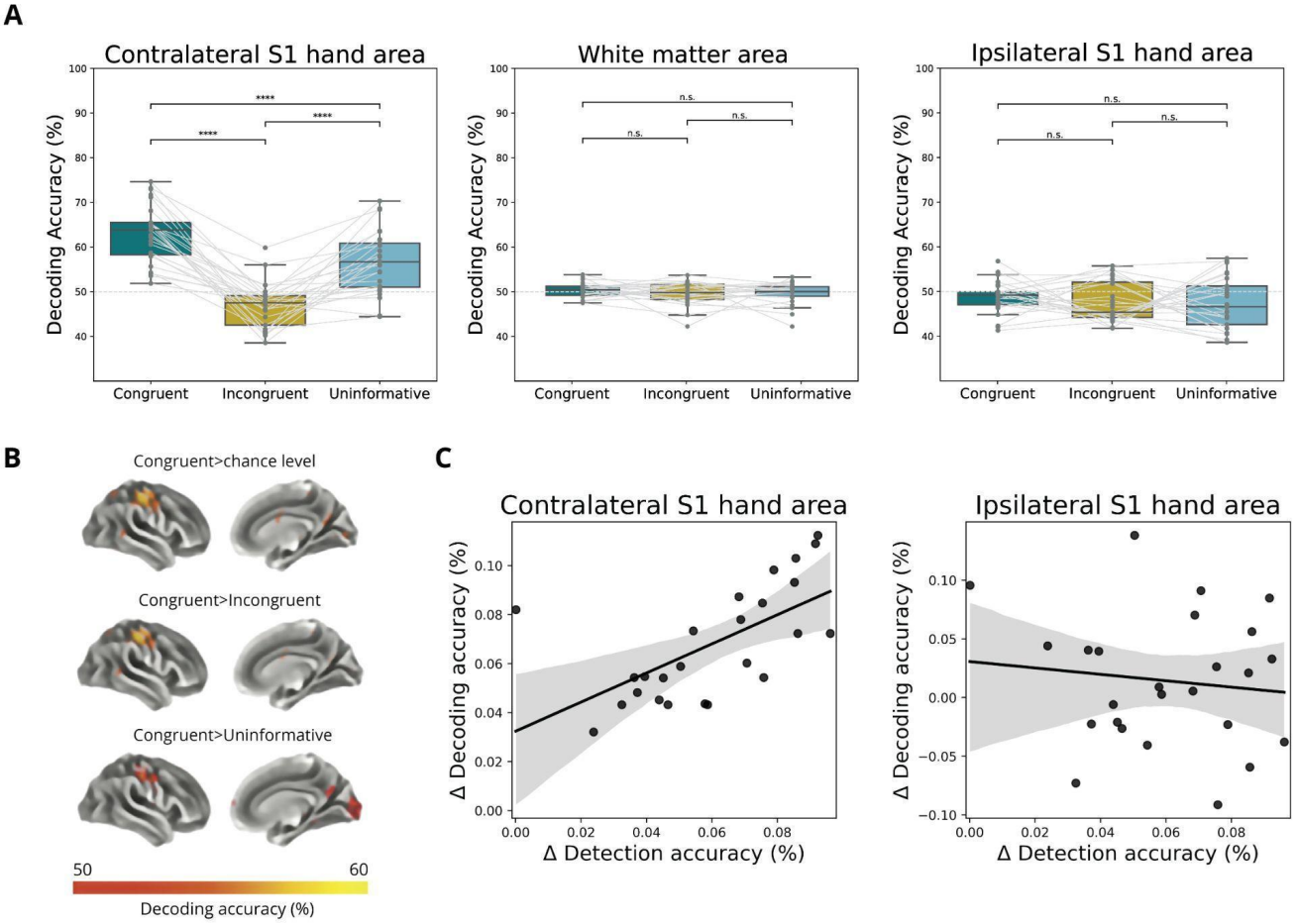

Figure 3 | Multi-voxel decoding of stimulated finger and its relationship to behavioral performance

(A) Boxplots of decoding accuracies of a binary classifier (linear Support Vector Machine; SVM) used to decode stimulated finger (ring finger versus thumb) based on beta estimates from first-level GLMs associated with vibrotactile stimulation events. Single-participant-results are visualized by gray lines. Decoding accuracies of the congruent (63.067±1.311%, $p < .001$) and the uninformative conditions (56.51±1.419%, $p<0.001$) but not of the incongruent condition (49.872±1.003%, $p=0.4$; all values mean±SEM) were significantly greater than chance level in the contralateral S1 hand area. Decoding accuracies for the ipsilateral S1 hand and for the white matter areas were not significantly different from chance level ($p>0.4$; Suppl. Table 3; see Materials and Methods for empirical chance level and p-value calculations). A repeated-measures two-way ANOVA confirmed a significant interaction effect of experimental condition and area ($F_{4,96} = 29.847$, $p<0.0001$, $\eta^2 = 0.294$). Decoding accuracies in the contralateral S1 hand area were significantly higher for the congruent condition as compared to incongruent ($p<0.0001$) and uninformative conditions ($p<0.0001$) while those for the ipsilateral S1 hand and for the white matter areas did not significantly differ between experimental conditions ($p>0.65$). Pairwise t-tests with post-hoc Bonferroni correction are conducted between experimental conditions (significance indicated by stars: n.s.: non-significant, **** $p < 0.0001$). **(B)** Top row: Searchlight decoding accuracies for the congruent condition (one-tailed t-test against chance-level, FWE-corrected with $p<0.05$). Second and third rows: One-sided t-tests between searchlight decoding results from congruent and the incongruent conditions, and from the congruent and the uninformative condition, respectively (FWE-correction, $p<0.05$). The largest cluster was located in the contralateral S1 hand area for all comparisons. Further significant clusters were found for the congruent > incongruent and congruent > incongruent comparisons in visual and default mode regions. **(C)** Robust linear regression revealed a significant relationship between an increase in behavioral detection accuracies and an increase of decoding accuracies from the uninformative to the congruent condition for the contralateral S1 hand area (Adjusted $R^2 = 0.626$, $p<0.001$, estimated regression slope (95% CI): 0.594 (0.31,0.82), but not for the ipsilateral S1 hand area (right-hand side panel; Adjusted $R^2 = -0.118$, $p=0.575$, estimated regression slope (95% CI): -0.272 (-0.49,0.22). Shaded areas visualize the 95% confidence intervals around the line of best fit. Decoding results show averaged accuracies over balanced 10-fold cross-validation.

Expectation induces somatotopic activity in contralateral S1

Recent studies have shown that the primary somatosensory cortex can be activated even in the absence of incoming sensory stimulation, for instance during touch observation or tactile imagery [25, 26, 49, 56]. It is, however, not known if probabilistic cues elicit somatotopic activity patterns in S1, and if such patterns relate to BOLD activity patterns from bottom-up vibrotactile stimulation and to behavioral discrimination performance. To assess this, we analyzed the BOLD activity for the period between visual cue display and vibrotactile stimulation ('delay period', Fig. 1C). We classified these periods as 'informative' when they followed a ring finger or a thumb cue and as 'uninformative' when they followed an informative visual cue (square in the display center). The uninformative delay periods served as a control condition and were separated into two groups based on the succeeding vibrotactile stimulation site (ring finger or thumb). Univariate contrasts of BOLD activity during informative delay periods after a ring finger or thumb cue revealed two distinct clusters of voxels within the contralateral S1 hand area, with peak t-values located proximal to the peak t-values associated with vibrotactile stimulation of the respective finger (Fig. 4A). We found that BOLD activity during informative delay periods was increased within the area of the cued finger and concurrently suppressed within the area of the non-cued finger, thus revealing a somatotopic organization of BOLD activity (Fig. 4B, left panel). In contrast, BOLD activity during uninformative delay periods revealed no such organization (Fig. 4B, right panel).

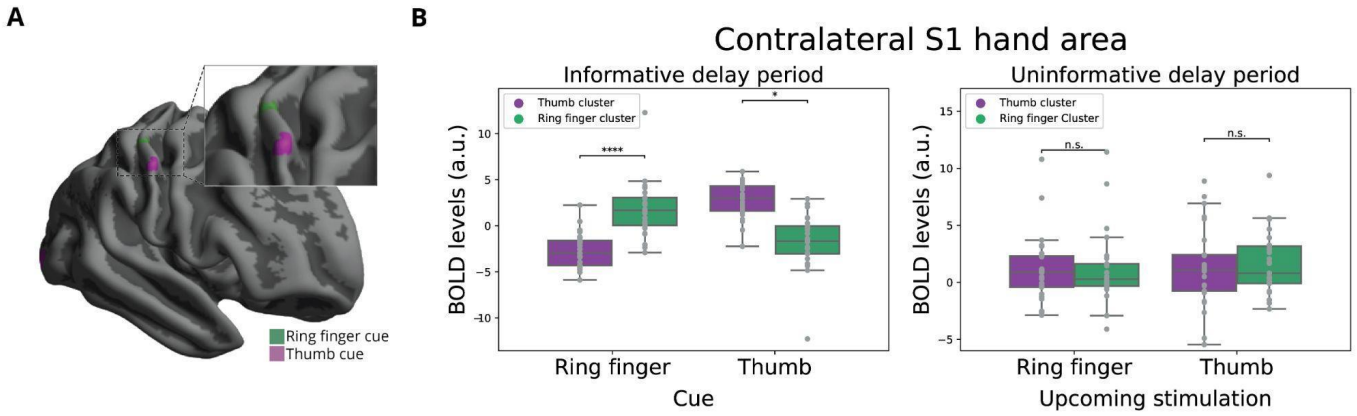

Figure 4 | BOLD activity for cued finger during the delay period (i.e prior to vibrotactile stimulation)

(A) Contralateral S1 regions activated after display of a ring finger cue (green) or a thumb cue (purple) during the informative delay period. Contrasting informative delay periods following ring finger versus thumb cues revealed two distinct clusters in close proximity to the ring finger and thumb representation associated with vibrotactile stimulation (MNI coordinates ring finger cue: 44 –24 60, thumb cue: 54 –14 50; t>=7.25, FWE corrected, p<0.05). **(B)** BOLD activity levels during the informative delay period revealed increased activation within the contralateral ring finger area with concurrent suppression of BOLD activity within the thumb cluster following ring finger cues and increased BOLD activity in the thumb cluster and concurrent suppression of BOLD activity in the ring area following thumb cues. Post hoc tests of a 2x2x2 way repeated measures ANOVA with Delay period category x Cluster x Cue condition revealed significant differences between the BOLD levels associated with finger versus thumb cues in both clusters for the informative delay period (p<0.01, t > -2.98) but no such significant differences for the uninformative period (p > 0.258, t > 0.0508). Single-participant-results are visualized by gray dots. n.s.: non-significant, * p < 0.01, *** p < 0.0001.

To assess the information content of the BOLD activity during the delay period we used a linear classifier to decode cued finger (ring finger cue versus thumb cue) from beta estimates obtained from the informative delay period. As a control we used a linear classifier to decode upcoming stimulation site (ring finger versus thumb) from beta estimates obtained from the uninformative delay period (Materials and Methods). We found that decoding accuracies for the informative delay period were significantly higher than chance level in the contralateral but not the ipsilateral S1 hand area (Fig. 5A). Decoding accuracies for the uninformative delay period were not significantly different than chance level in both cases, but significantly different from decoding accuracies of the informative delay period in the contralateral S1 hand area.

We then asked if within the S1 hand area the representations of tactile stimuli generalized from delay periods to those from vibrotactile stimulation. To this end, a linear classifier was trained on beta estimates obtained from the delay period and tested on beta estimates obtained from vibrotactile stimulation. Training the classifier on beta estimates of the informative delay period extracted from the contralateral but not those extracted from the ipsilateral S1 hand area revealed decoding accuracies significantly above chance level (Fig. 5B). Training the decoder on non-informative delay periods was associated with decoding accuracies around chance level for both ipsilateral and contralateral hand areas.

When comparing the improvement of behavioral detection accuracies between uninformative and congruent vibrotactile stimulation to improvements in decoding accuracy between uninformative and informative delay periods, we found a significant correlation in the contralateral S1 hand but not in the ipsilateral S1 hand area, suggesting the behavioral relevance of somatotopic activity patterns before vibrotactile stimulus onset, even though the association was weaker when compared to improvements during vibrotactile stimulation (Fig. 5C). Thus, expectation of vibrotactile stimulation to a finger elicits somatotopic BOLD activity, the activity is informative for decoding the cued finger and similar to that elicited by vibrotactile stimulation in that their multivoxel representations generalize.

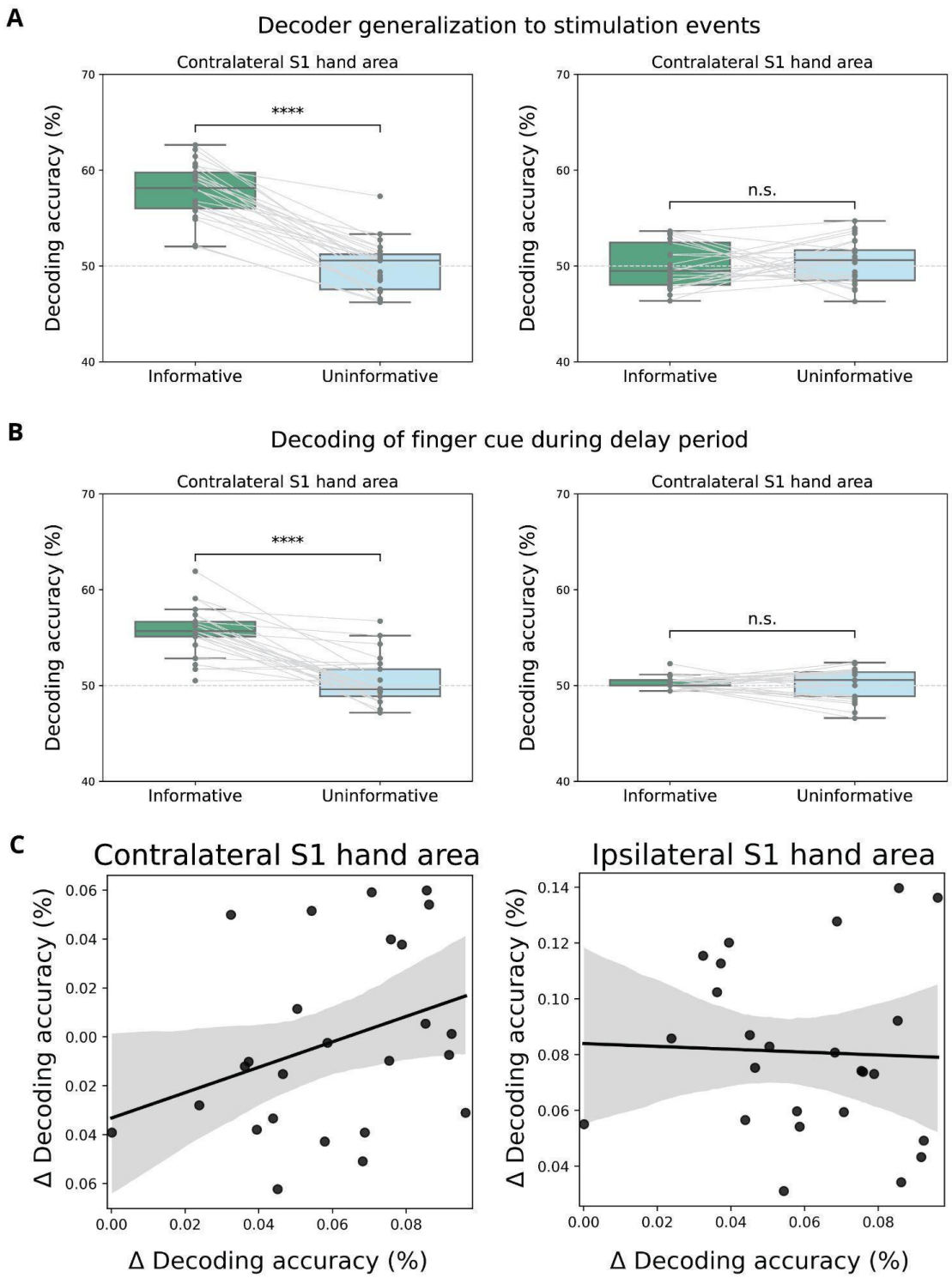

Figure 5 | Group level results of decoding the cued stimulation site from neural activity in contra- and ipsilateral S1 hand area during the delay period. **(A)** Decoding the finger cue (ring finger versus thumb cue) with a linear SVM classifier resulted in significantly higher than chance level accuracies in contralateral S1 hand area for first-level GLM beta estimates from the informative delay period (57.3±2.8%, p<0.0001). Decoding upcoming stimulation site from the uninformative delay period used as a control condition resulted in accuracies which were not significantly different from chance level (49.02±5.5, p=0.72). The same decoding analysis yielded accuracies around chance-level for both informative and uninformative delay periods for beta estimates extracted from the ipsilateral S1 hand area (49.45±4.71 and 50.12±2.5%, respectively; p>0.62; all values mean±SEM). A two way repeated measures ANOVA revealed a significant interaction for factors condition x area with $F_{1,24} = 63.26$, $p<0.0001$, $\eta^2 = 0.423$. Pairwise t-tests with post-hoc Bonferroni correction are conducted between experimental conditions (significance indicated by stars: n.s.: non-significant, **** p < 0.0001). **(B)** A linear SVM classifier was trained on either the informative delay period (ring finger cue versus thumb cue) or the uninformative delay period (upcoming ring finger stimulation versus upcoming thumb stimulation) and applied to the vibrotactile stimulation period (prediction of ring finger versus thumb stimulation). Decoding accuracies from the contralateral S1 hand area were only significantly higher than chance level when the decoder was trained on beta estimates from the informative delay period (56.92±3.7%, p < 0.0001) but not when it was trained on beta estimates from the uninformative delay period (48.93±4.8%, p>0.7). Using a linear classifier with the same test-train scheme to

decode stimulated finger from beta estimates of the ipsilateral S1 hand area resulted in accuracies which did not significantly differ from chance level for neither condition (50.1±1.2% and 49.3±3.2%, respectively; p>0.6). A two way repeated measures ANOVA revealed a significant interaction for factors condition x area with $F_{1,24}$ = 35.38524, p<0.0001, η^2 = 0.308. **(C)** Robust linear regression revealed a significant relationship between an increase in behavioral detection accuracies and an increase of decoding accuracies from the uninformative to the informative delay periods for the contralateral S1 hand area (Adjusted R^2 = 0.074, p=0.039, 95% CI =[0.031,1.047] for a regression slope of 0.539 but not for the ipsilateral S1 hand area (right-hand side panel; Adjusted R^2 = -0.032, p=0.728, 95% CI =[-0.949,0.672] for a regression slope of -0.138. Shaded areas visualize the 95% confidence intervals around the line of best fit. Decoding accuracies: mean±SEM over participants. Single-participant-results are visualized by gray lines. Decoding results show averaged accuracies over balanced 10-fold cross-validation.

Discussion

In recent work, expectation has been found to facilitate perceptual performance in a wide range of behavioral tasks, while sensory stimuli which match prior expectations are associated with decreased BOLD levels in early sensory areas [4, 2, 11, 21, 5]. This seemingly surprising finding has been reconciled by the demonstration of higher decoding accuracies of BOLD activity associated with congruent stimuli and explained with a better signal to noise ratio [4, 2, 11].

Most existing studies on the integration of prior information with sensory input have focused on the visual domain. We focus on the somatosensory areas, as they provide a macroscopic, supra-voxel gradient which allows for the dissociation of distinct finger regions as accessible by fMRI and thus provide an ideal basis to assess how prior information modulates tactile stimulus representations. We asked how prior information influences the representation of vibrotactile stimuli both before and during stimulation events and how these representations relate to the behavioral performance of participants. We designed a vibrotactile discrimination study where we showed that vibrotactile stimuli congruent with prior information are associated with significant improvements of behavioral detection performance, and, consistent with findings on the early visual areas, are associated with a concurrent suppression of the BOLD level in the contralateral S1 hand area.

By decoding stimulated fingers (ring finger versus thumb) we found that despite the suppression of BOLD level, decoding accuracies obtained by a linear classifier were highest for congruent tactile stimuli as compared to incongruent stimuli or stimuli for which no prior information was provided to participants. Importantly, we found that the behavioral improvements and the improvements of decoding performance from the uninformative to the congruent condition were related, suggesting the behavioral relevance of the decoding accuracy associated with the BOLD signal from the contralateral S1. We did not find decoding accuracies to be significantly higher than chance level in any of the control areas, including the ipsilateral and contralateral secondary somatosensory cortices. This is consistent with recent studies where individual finger representations could not be resolved in S2 areas even with 7T fMRI [53].

Whole brain decoding by means of a searchlight approach (Materials and Methods) confirmed that the effects of prior information were largely confined to S1, with peak decoding accuracies being located proximal to univariate peak BOLD activity and the distinct somatotopic representations of ring finger and thumb. Thus, our results suggest that the behavioral improvements through prior information are associated with higher separability of stimulus representations by exploiting the somatotopic organization of contralateral S1. Our findings provide evidence for the integration of prior information early in the somatosensory processing stages, within sensory areas where the activity of neural populations could be 'tuned' distinctly for the expected tactile stimulus. This finding is surprising, as traditionally it has been thought that the integration of prior expectations might take place in higher order regions associated with decision making processes [55] and that S1 is chiefly involved in the processing of afferent tactile input. Yet although modality-based discrimination of tactile versus auditory stimuli have revealed category-specific

information in somatosensory association areas outside of S1 [25], we did not find any significant decoding accuracies in regions outside of S1, such as the superior parietal cortex or intraparietal sulcus which are considered somatosensory association areas. A possible explanation for this discrepancy lies in differences in behavioral design and differences in encoding of between versus within-modality stimuli - somatosensory association areas might be involved in modality-specific dissociation but not mainly in the fine grained dissociation of distinct fingers as associated with the primary somatosensory cortex.

The finding that prior information is integrated during early stages of perceptual processing has led to the question if the relevant early sensory areas can be activated by top-down information even before stimulus onset. Previous studies of the visual and auditory domains have revealed that expectation increases baseline activity of category-specific regions, hypothesizing that this allows for an efficient subsequent processing of the predicted stimuli through the activation of neural populations tuned for the upcoming stimuli [21, 23, 11, 12]. Indeed, such anticipatory activity has been associated with behavioral performance for task-relevant stimuli congruent with subjects' expectations [11, 12]. Even though previous studies have shown that S1 exhibits somatotopic activity in the absence of incoming tactile stimuli [56], it had not yet been shown how such activity is related to task performance, how the BOLD signal is modulated in the absence of bottom-up tactile information for specific finger areas and based on prior probabilistic cues. Here, we found that informative but not uninformative probabilistic finger cues induce anticipatory activity patterns in the contralateral S1 hand region and that the BOLD levels during this 'delay period' are suppressed in the area associated with the non-cued finger. In addition, we found that ring finger and thumb cues could be decoded from BOLD activity after an informative cue (ring finger or thumb cue), and that the performance of the linear decoder was related to the upcoming detection performance of the participants. A subsequent decoding analysis confirmed that these anticipatory activity patterns were informative and similar to those induced by somatosensory stimuli. In summary, our results provide evidence that prior information can drive somatotopic activity in early somatosensory areas even in the absence of tactile stimuli, and that this activity is task relevant. This findings adds to the recent literature which indicates that S1 is involved in higher order processing of tactile information [25, 26, 56] and that it does so by the exploitation of its somatotopic organization [56].

Anticipatory activity in both early and late sensory areas has been associated with a variety of top-down cognitive processes, such as mental imagery or feature-based attention [24]. With respect to the somatosensory domain recent studies have demonstrated that both tactile imagery as well as motor planning evoke informative activity patterns in somatosensory areas [25, 26, 56]. It remains unclear, however, how and if these activity patterns differ depending on the involved top-down processes such as planning, attention of expectation. While it has been shown for instance that motor preparation elicits somatotopic activity in S1 similar to the activity induced by motor execution, neural representations associated with mental imagery have only been found to allow for the dissociation of imagery modality (e.g. tactile versus auditory) but not for imagery content [25]. Hence, the assessment of the differences between different categories of anticipatory neural activity both in somatosensory areas and areas associated with other stimulus modalities constitutes a promising future line of research. It is important to note that, as we did not make an explicit distinction between spatial expectation and spatial attention in the current study, the contributions of each of the two mechanisms to the anticipatory neuronal activity cannot be distinguished here.

What is the relevance of anticipatory activity induced by probabilistic cues? It has been argued that anticipatory activity could increase sensory gain, thus for instance preparing motor action. In line with this argument we find that anticipatory neural activity in S1 is related to upcoming behavioral performance, thus

indicating potentially a similar role of anticipatory activity for the detection and dissociation of tactile stimuli. In summary, we find that vibrotactile stimuli matching prior information leads to a better dissociation of tactile representations in S1, that this improvement of decoding accuracy is related to behavioral performance and associated with a suppression of the BOLD level for congruent stimuli. In addition, our results indicate that prediction is not time-locked to stimulus onset and thus our results expand on previous findings insofar as tactile information is shown to induce somatotopic activity in S1. Importantly, we show that this activity is based on a finger specific modulation of the BOLD signal and predictive of the upcoming task performance.

Materials and Methods

Participants, Power, Ethics. A convenience sample of 25 healthy volunteers (17 males, 8 females, age 26 ± 4 years (mean ± SD); all right handed) participated in the study. The sample size was an extension of sample sizes used by previous neuroimaging studies of the effect of prior information on sensory representations [2]. Participants' informed consent was obtained according to the Declaration of Helsinki prior to study onset. Ethical approval was granted by the Kantonale Ethikkommission Zürich (KEK-2015-0537).

Experimental design. After familiarization in a mock-scanner, participants performed vibrotactile detection tasks in a functional magnetic resonance imagining (fMRI) scanner during 2 sessions on two subsequent days. Each fMRI imaging session consisted of four imaging runs. Each such run (~10 minutes) consisted of 40 trials and was preceded by a psychophysical staircase procedure (~7 minutes). In addition, day 1 began with functional localizer runs (2 runs of each 10 minutes) and a structural scan was obtained for each participant at the end of day 2 (~7 minutes), resulting in a duration of ~1.5-2 hours for each fMRI imaging session.

Vibrotactile stimulation. Custom-made, MR compatible piezo-electric devices (Dancer Design, UK) were used to deliver stimulation to the fingertips of participants' ring finger and thumb of the left hand. These fingers were chosen because of their anatomically distinct representation in S1 [16, 50]. Stimulators were fixated on the fingers using Velcro straps to ensure good contact with the skin throughout the experiment without compromising blood supply of participants. A pulsed sinusoid with 5 bursts per stimulation, a frequency of 50 Hz, 40ms gaps and a duration of 3.8 seconds was employed for stimulation throughout the entire study. Visual input was displayed on a screen visible to participants through a mirror placed on the head coil. Stimulation and display were controlled by in-house scripts implemented in MATLAB [26] and functions from the Psychophysics Toolbox [27, 28, 29]. Two interleaved one-up one-down staircases were employed prior to each imaging run, to determine vibrotactile detection thresholds separately for the ring finger and thumb of the left hand of each participant. Each staircase started at 1 Volt stimulation intensity and consisted of 7 trials per finger in a randomized order where participants had to indicate on which finger they perceived the stimulation. To ensure an experimental environment akin to the main experiment, staircases were conducted inside the scanner while echo-planar images (EPIs) were acquired, but the corresponding MR scans were discarded at the end of the scanning session. For the following imaging session vibrotactile stimuli were presented around the participants' detection threshold with stimulation intensities sampled for each finger individually from a skew-normal distribution with a skewness of 0.5 and

a kurtosis of 4, while the mode of the distribution was set to the vibrotactile detection threshold of that finger (Fig. 1B).

Experimental imaging runs and behavioral tasks. During each imaging run participants performed a vibrotactile detection task with 40 trials, resulting in a total of 320 trials over 8 imaging runs in two days. Each vibrotactile detection trial began with the display of prior visual information (also referred to as a probabilistic cue; 1s duration). Next, in the vibrotactile stimulation period (3.8s), participants received stimulation to either the thumb or ring finger of the left hand. Finally, there was a response period (2s) where participants indicated the perceived vibrotactile stimulation site: ring finger, thumb or none in case they could not detect the stimulation. The three parts of the trial were separated by delay intervals of variable lengths (3.5-4.5s and 2.5-3.5s, respectively), and also the different trials were separated by delay intervals of variable lengths sampled from an uniform distribution (1-2s; Fig. 1C). During the delay intervals, participants were instructed to focus on a fixation cross.

The probabilistic cue (a green square on a black background) appeared either on the left, right or center of the screen. A square on the left indicated that stimulation was likely (80% chance) to be applied to the left ring finger (ring finger cue), while a square on the right indicated that stimulation was likely (80% chance) to be applied to the thumb (thumb cue). A square in the middle implied that stimulation to the thumb or ring finger was equally likely (uninformative cue). Note that the visual cue location was spatially consistent to the position of the cued finger of participant's left hand thus ensuring an intuitive mapping for the participants.

Trials where the stimulated finger matched the cue were classified as belonging to the 'congruent' experimental condition (thumb cue – stimulation of thumb; ring finger cue – stimulation of ring finger), while trials where the stimulated finger was contrary to the cue were classified as belonging to the 'incongruent' experimental condition (thumb cue – stimulation of ring finger; ring finger cue – stimulation of thumb). The trials with the uninformative cue formed the 'uninformative' experimental condition. Of the total of 320 trials, 172 fell into the congruent category, 44 into the incongruent category and 104 into the uninformative category.

During the response period, participants could select from three response options ("Ring finger", "Thumb", or "None") with their right hand through key presses on a button box. The response options changed color upon selection, and their arrangement was randomized to prevent preparatory motor artifacts prior to the response period. In addition, the order of experimental conditions (congruent, incongruent, uninformative) was randomized for each run while it was ensured that each experimental condition contained the same number of ring finger and thumb trials.

Statistical analysis of the behavioral task. The behavioral detection accuracy (Fig. 2A) was calculated as the fraction of correctly recognized stimulation sites over all vibrotactile stimulation events over the 8 runs. Statistical analyses were performed using the R 4.2.1 statistical software [51]. Post hoc Bonferroni corrected p-values for two-sided pairwise t-tests were also included.

We performed a robust regression analysis (with robustbase in R) to assess if the improvement of behavioral detection accuracy and the improvement of decoding accuracy observed for congruent stimuli were related. To this end, the independent variable was calculated as the difference between behavioral accuracy for the congruent stimuli and the behavioral accuracy for uninformative stimuli for each subject. The dependent variable was calculated as the difference between decoding accuracy for the congruent stimuli and the decoding accuracy for uninformative stimuli for each subject either based on the BOLD signal in the

contralateral S1 region (Fig. 3C, left panel) or the ipsilateral S1 region (Fig. 3C, right panel). Next we assessed the relationship between the improvement of behavioral detection accuracy for congruent stimuli and the decoding accuracy of the informative delay period to assess the behavioral relevance of the BOLD signal induced by a finger cue prior to vibrotactile stimulation. Here, the independent variable was calculated as the difference between the decoding accuracy for the informative delay period minus the decoding accuracy for the uninformative delay period for each subject. The robust regression analysis was again performed for both the contralateral S1 region (Fig. 5C, left panel) and the ipsilateral S1 region (Fig. 5C, right panel).

Functional Localizer. A functional localizer was obtained within 2 runs from each participant on day 1 prior to the start of the imaging runs of the main experiment. Fingers were stimulated with a clearly perceivable, suprathreshold vibrotactile stimuli (4 Volts stimulation intensity, 4s duration). Each finger was stimulated 15 times with variable interstimulus intervals between the stimulation periods. The marsbar ROI toolbox (http://marsbar.sourceforge.net) was used to extract ring finger and thumb region of interest masks for each participant based on the significant cluster of activity ($p<0.05$) in contralateral S1 from a vibrotactile stimulation to resting baseline contrast.

fMRI data acquisition. Functional images were acquired on a Philips Ingenia 3T with a fifteen element head coil. The T2*-weighted gradient-echo transversal EPI sequences were acquired with a spatial resolution of $2.75\times2.75\times3.3$ mm^3, TR/TE = 2500ms/35ms and an epi-factor of 39 and a sense acceleration factor of 2. The 40 acquired slices with no interslice gap were oriented parallel to the ACPC line. Anatomical images were acquired with a 1 mm×1 mm×1 mm spatial resolution, TR/TE = 8.38 ms/3.94 ms and a sense acceleration factor of 1.5 and sagittal orientation.

fMRI preprocessing and univariate analysis. The fMRI data was pre-processed using a standard pipeline (i.e., realignment, normalization, and smoothing) in FSL (v5.00; https://fsl.fmrib.ox.ac.uk/fsl/fslwiki/FSL). Realignment of the functional images was followed by skull stripping applied to the structural image with the brain extraction tool BET [30, 31]. Structural images were segmented with FAST [32] and the boundary based co-registration tool FLIRT [33, 34] was then used to co-register functional images to the structural image. Motion correction was applied using MCFLIRT [33, 34]. Spatial smoothing with a 3 mm full-width half maximum Gaussian kernel and a high-pass filter with a cut-off of 100 seconds were applied to the co-registered functional images. Finally, functional images were normalized to the MNI template space with FNIRT [35]. The preprocessed images were analyzed with a general linear model (GLM). We defined separate regressors for each vibrotactile stimulation and each delay period (period between visual cue display and vibrotactile stimulation). Visual cue display and the response period were each included as regressors of no interest, as were head motion parameters. Single-subject (first-level) beta estimates (regression coefficients) were obtained based on the double-gamma hemodynamic response function (canonical HRF) and its temporal derivatives. The first-level analysis resulted in activation images (beta maps) for each of the vibrotactile stimulation and each of the delay periods for each of the participants. Contrasts for main effects and interactions were defined at the first level and employed for the group-level (second-level) analysis. Results are reported at $p < 0.05$ and familywise error (FWE) corrected at the voxel level based on the Threshold-Free Cluster Enhancement (TFCE; Smith and Nichols, 2009). BOLD level analysis (Fig. 2C) was performed by averaging the beta estimates for all stimulation events of a condition over all voxels.

Regions of interest. Contralateral and ipsilateral S1 hand areas were defined with masks as described in a previous study [37] and employed for ROI-based decoding analysis as well as for an assessment of BOLD levels associated with the three different experimental conditions. Further regions of interest were extracted

in MNI space with probabilistic cytoarchitectonic masks from the anatomy toolbox [38] and used as control regions for the ROI-based decoding analysis. In particular, we extracted masks for the secondary somatosensory cortices (S2; 2872 voxels), the primary motor cortex (M1; 4321 voxels); the primary visual cortex (V1; 1802 voxels) and for white matter regions (xyz voxels). The marsbar ROI toolbox (http://marsbar.sourceforge.net) was used to extract ring finger and thumb region of interest masks for each participant based on the significant cluster of activity ($p<0.05$) in contralateral S1 from a vibrotactile stimulation to resting baseline contrast and peak voxel coordinates for the vibrotactile stimulation of the fingers of each participant. These masks were employed to assess the modulation of the BOLD signal as a function of the finger cue during the delay period.

Region of interest decoding. Beta estimates within the respective ROI were extracted from the beta-maps obtained by the first-level GLM (stimulation events or delay periods each 320 beta-maps per subject) for the subsequent decoding analysis. The decoding analysis was implemented with a linear Support Vector Machine with MATLAB's fitcsvm function [27]. The linear SVM was employed to predict stimulated finger (ring finger or thumb) for each experimental condition (congruent, incongruent or uninformative). To match the number of voxels between different ROIs and to thus make results of the decoding analysis comparable, 300 voxels were randomly subsampled from each ROI for each iteration of a 10-fold cross-validation. Reported decoding accuracies are cross-validation accuracies averaged over 1000 rounds of repeated cross-validation, and with a default setting for the cost parameter of C=1. The decoding was balanced by subsampling across each experimental condition to obtain the same number of stimulation events per condition. Decoding labels were permuted to assess the significance of decoding accuracies and the p-value decoding versus chance level was calculated as the fraction of decoding accuracies from the permuted dataset larger than accuracies obtained from the original dataset based on 1000 permutations [40].

Whole-brain searchlight decoding. A whole-brain searchlight analysis was employed to decode vibrotactile stimuli across the entire brain. To this end we implemented with the pyMVPA toolbox a decoding approach where a linear SVM (C=1) was applied one by one to each voxel and its surrounding sphere (radius of 1 voxel). The linear classifier was employed to predict stimulated fingers (ring finger or thumb) based on the 320 beta maps corresponding to the 320 stimulation events. The decoding was balanced by subsampling across each experimental condition to obtain the same number of stimulation events per condition. This approach resulted in a whole-brain accuracy map where the decoding accuracy is ascribed to the voxel in the center of the sphere. To obtain group-level statistics a t-test across participants was performed against 50% chance level or between experimental conditions and the group-level accuracy maps were FWE corrected ($p>0.05$). Searchlight accuracy maps were plotted with the connectome workbench (Fig. 3B) [44].

References

[1] Ouden, H. E. M. D., Daunizeau, J., Roiser, J., Friston, K. J. and Stephan, K. E. (2010). Striatal Prediction Error Modulates Cortical Coupling. *Journal of Neuroscience*, 30(9), pp. 3210-3219.

[2] Kok, P., Jehee, J. F. and De Lange, F. P. (2012). Less Is More: Expectation Sharpens Representations in the Primary Visual Cortex. *Neuron*, 75(2), pp. 265-270.

[3] Turk-Browne, N. B., Scholl, B. J., Johnson, M. K. and Chun, M. M. (2010). Implicit Perceptual Anticipation Triggered by Statistical Learning. *Journal of Neuroscience*, 30(33), pp. 11177-11187.

[4] Egner, T., Monti, J. M., and Summerfield, C. (2010). Expectation and Surprise Determine Neural Population Responses in the Ventral Visual Stream. *Journal of Neuroscience*, 30(49), pp. 16601-16608.

[5] Richter, D., Ekman, M. and Lange, F. P. D. (2017). Suppressed sensory response to predictable object stimuli throughout the ventral visual stream. pre-print, *bioRxiv*.

[6] Schellekens, W., Wezel, R. J. A. V., Petridou, N., Ramsey, N. F., and Raemaekers, M. (2014). Predictive coding for motion stimuli in human early visual cortex. *Brain Structure and Function*, 221(2), pp. 879-890.

[7] Lee, T. S. and Mumford, D. (2003). Hierarchical Bayesian inference in the visual cortex. *Journal of the Optical Society of America*, 20(7), p. 1434.

[8] Kaposvari, P., Kumar, S. and Vogels, R. (2016). Statistical Learning Signals in Macaque Inferior Temporal Cortex. *Cerebral Cortex*, 28(1), pp. 250-266.

[9] Meyer, T. and Olson, C. R. (2011). Statistical learning of visual transitions in monkey inferotemporal cortex. *PNAS*, 108(48), pp. 19401-19406.

[10] Turk-Browne, N. B., Scholl, B. J., Chun, M. M. and Johnson, M. K. (2009). Neural Evidence of Statistical Learning: Efficient Detection of Visual Regularities Without Awareness. Journal of Cognitive Neuroscience, 21(10), pp. 1934-1945.

[11] Kok, P., Failing, M. F. and Lange, F. P. D. (2014). Prior Expectations Evoke Stimulus Templates in the Primary Visual Cortex. *Journal of Cognitive Neuroscience*, 26(7), pp. 1546-1554.

[12] Kok, P., Mostert, P. and Lange, F. P. D. (2017). Prior expectations induce pre-stimulus sensory templates. *PNAS*, 114 (39), pp. 10473-10478.

[13] Preuschhof, C., Schubert, T., Villringer, A. and Heekeren, H. R. (2010). Prior Information Biases Stimulus Representations during Vibrotactile Decision Making. *Journal of Cognitive Neuroscience*, 22(5), pp. 875-887.

[14] Brouwer, Anne-Marie, and Jan BF Van Erp. "A tactile P300 brain-computer interface." *Frontiers in neuroscience* 4 (2010): 19.

[15] Bogacz, R., Brown, E., Moehlis, J., Holmes, P. and Cohen, J. D. (2006). The physics of optimal decision making: A formal analysis of models of performance in two-alternative forced-choice tasks. *Psychological Review*, 113(4), pp. 700-765.

[16] Martuzzi, R., Zwaag, W. V. D., Farthouat, J., Gruetter, R. and Blanke, O. (2012). Human finger somatotopy in areas 3b, 1, and 2: A 7T fMRI study using a natural stimulus. *Human Brain Mapping*, 35(1), pp. 213-226.

[17] Hernandez, A., Zainos, A. and Romo, R. (2000). Neuronal correlates of sensory discrimination in the somatosensory cortex. *PNAS*, 97(11), pp. 6191-6196.

[18] Luna, R., Hernandez, A., Brody, C. D. and Romo, R. (2005). Neural codes for perceptual discrimination in primary somatosensory cortex. *Nature Neuroscience*, 8(9), pp. 1210-1219.

[19] Penfield, W. and Boldrey, E. (1937). Somatic Motor And Sensory Representation In The Cerebral Cortex Of Man As Studied By Electrical Stimulation. *Brain*, 60(4), pp. 389-443.

[20] Summerfield, C., Trittschuh, E. H., Monti, J. M., Mesulam, M.-M. and Egner, T. (2008). Neural repetition suppression reflects fulfilled perceptual expectations. *Nature Neuroscience*, 11(9), pp. 1004-1006.

[21] Bell, A. H., Summerfield, C., Morin, E. L., Malecek, N. J. and Ungerleider, L. G. (2016). Encoding of Stimulus Probability in Macaque Inferior Temporal Cortex. *Current Biology*, 26(17), pp. 2280-2290.

[22] Kumar S., Kaposvari P. and Vogels R. (2017). Encoding of predictable and unpredictable stimuli by inferior temporal cortical neurons. *Journal of Cognitive Neuroscience*, 29, pp. 1445-1454.

[23] Esterman, M. and Yantis, S. (2010). Perceptual expectation evokes category-selective cortical activity. *Cerebral Cortex*, 20(5), pp.1245-53.

[24] 199 - Liu, Y., Bengson, J., Huang, H., Mangun, G.R. and Ding, M. (2016). Top-down Modulation of Neural Activity in Anticipatory Visual Attention: Control Mechanisms Revealed by Simultaneous EEG-fMRI. *Cerebral Cortex*, 26(2), pp. 517-529.

[25] de Borst A. W. and de Gelder, B. (2017). fMRI-based Multivariate Pattern Analyses Reveal Imagery Modality and Imagery Content Specific Representations in Primary Somatosensory, Motor and Auditory Cortices. *Cerebral Cortex*, 27(8), pp. 3994-4009.

[26] de Borst AW, De Gelder B. Mental imagery follows similar cortical reorganization as perception: intra-modal and cross-modal plasticity in congenitally blind. Cerebral Cortex. 2019 Jul 5;29(7):2859-75.

[27] MATLAB, MATLAB and Statistics Toolbox Release 2016b, The MathWorks, Inc., Natick, Massachusetts, United States, 2016

[28] Brainard, D. (1997). The Psychophysics Toolbox. *Spatial Vision*, 10(4), pp. 433-436.

[29] Kleiner, M., Brainard, D., Pelli, D., Ingling, A., Murray, R. and Broussard, C. (2007). What's new in psychtoolbox-3, Pion Ltd., *Perception*, 36(14), pp. 1-16.

[30] Pelli, D. G. (1997). The VideoToolbox software for visual psychophysics: transforming numbers into movies. *Spatial Vision*, 10(4), pp. 437-442.

[31] Jenkinson, M., Pechaud, M., and Smith, S. (2005). MR-based estimation of brain, skull and scalp surfaces. Cold Spring Harbor Labs Journals, *Human Brain Mapping*, http://biorxiv.org/content/early/2016/01/14/029983

[32] Smith, S. M. (2002). Fast robust automated brain extraction. *Human Brain Mapping*, 17(3), pp. 143-155.

[33] Zhang, Y., Brady, M. and Smith, S. (2001). Segmentation of brain MR images through a hidden Markov random field model and the expectation-maximization algorithm. *IEEE Transactions on Medical Imaging*, 20(1), pp. 45-57.

[34] Jenkinson, M., and Smith, S. (2001). A global optimisation method for robust affine registration of brain images. *Medical Image Analysis*, 5(2), pp. 143-156.

[35] Jenkinson, M., Bannister, P., Brady, M. and Smith, S. (2002). Improved Optimization for the Robust and Accurate Linear Registration and Motion Correction of Brain Images. *NeuroImage*, 17(2), pp. 825-841.

[36] Andersson, J., Jenkinson, M. and Smith, S. (2014). Non-linear registration, aka spatial normalisation. *Cold Spring Harbor Labs Journals: FMRIB Technical Report*.

[37] Kikkert, S., Mezue, M., Slater, D. H., Johansen-Berg, H., Tracey, I. and Makin, T. R. (2017). Motor correlates of phantom limb pain. *Cortex*, 95, pp. 29-36.

[38] Eickhoff, S. B., Stephan, K. E., Mohlberg, H., Grefkes, C., Fink, G. R., Amunts, K. and Zilles, K. (2005). A new SPM toolbox for combining probabilistic cytoarchitectonic maps and functional imaging data. *NeuroImage*, 25(4), pp. 1325-1335.

[39] Shirer, W. R., Ryali, S., Rykhlevskaia, E., Menon, V. and Greicius, M. D. (2011). Decoding Subject-Driven Cognitive States with Whole-Brain Connectivity Patterns. *Cerebral Cortex*, 22(1), pp. 158-165.

[40] Kassraian-Fard, P.K., Matthis, C., Balsters, J.H., Marloes H. Maathuis and Wenderoth, N. (2016). Promises, Pitfalls, and Basic Guidelines for Applying Machine Learning Classifiers to Psychiatric Imaging data, with Autism as an example. *Frontiers in Psychiatry*, 7.

[41] Kassraian-Fard P, Pfeiffer M, Bauer R. A generative growth model for thalamocortical axonal branching in primary visual cortex. PLoS computational biology. 2020 Feb 13;16(2):e1007315.

[42] Ruddy K, Balsters J, Mantini D, Liu Q, Kassraian-Fard P, Enz N, Mihelj E, Chander BS, Soekadar SR, Wenderoth N. Neural activity related to volitional regulation of cortical excitability. Elife. 2018;7.

[43] Ojala, M. and Garriga, G. C. (2009). Permutation Tests for Studying Classifier Performance. *Ninth IEEE International Conference on Data Mining*.

[44] Kriegeskorte, N. (2008). Representational similarity analysis? connecting the branches of systems neuroscience. *Frontiers in Systems Neuroscience*.

[45] Kriegeskorte, N., Goebel, R. and Bandettini, P. (2006). Information-based functional brain mapping. *PNAS*, 103(10), pp. 3863-3868.

[46] Hanke, M., Halchenko, Y. O., Sederberg, P. B., Hanson, S. J., Haxby, J. V. and Pollmann, S. (2009). PyMVPA: a Python Toolbox for Multivariate Pattern Analysis of fMRI Data. *Neuroinformatics*, 7(1), pp. 37-53.

[47] Marcus, D. S., Harwell, J., Olsen, T., Hodge, M., Glasser, M. F., Prior, F. and Essen, D. C. V. (2011). Informatics and Data Mining Tools and Strategies for the Human Connectome Project. *Frontiers in Neuroinformatics*, 5.

[48] Ramachandran, P. and Varoquaux, G. (2011). Mayavi: 3D Visualization of Scientific Data. *Computing in Science and Engineering*, 13(2), pp. 40-51.

[49] Panchuelo, R.M.S., Ackerley, R., Glover, P.M., Bowtell, R.W., Wessberg, J., Francis, S.T. and McGlone, F. (2016). Mapping quantal touch using 7 Tesla functional magnetic resonance imaging and single-unit intraneural microstimulation. *Elife*, *5*, p.e12812.

[50] Sanchez-Panchuelo, Rosa Maria, Susan Francis, Richard Bowtell, and Denis Schluppeck. "Mapping human somatosensory cortex in individual subjects with 7T functional MRI." *Journal of neurophysiology* 103, no. 5 (2010): 2544-2556.

[51] Kuehn E, Mueller K, Turner R, Schütz-Bosbach S. The functional architecture of S1 during touch observation described with 7 T fMRI. Brain Structure and Function. 2014 Jan;219(1):119-40.

[52] Ejaz N, Hamada M, Diedrichsen J. Hand use predicts the structure of representations in sensorimotor cortex. Nature neuroscience. 2015 Jul;18(7):1034-40.

[53] R Core Team (2012). R: A language and environment for statistical computing. R Foundation for Statistical Computing, Vienna, Austria. ISBN 3-900051-07-0, URL http://www.R-project.org/

[52] Gallivan JP, Johnsrude IS, Randall Flanagan J. Planning ahead: object-directed sequential actions decoded from human frontoparietal and occipitotemporal networks. Cerebral Cortex. 2016 Feb 1;26(2):708-30.

[53] Sanchez Panchuelo RM, Besle J, Schluppeck D, Humberstone M, Francis S. Somatotopy in the human somatosensory system. Frontiers in human neuroscience. 2018 Jun 12;12:235.

[54] Aitken F, Turner G, Kok P. Prior expectations of motion direction modulate early sensory processing. Journal of Neuroscience. 2020 Aug 12;40(33):6389-97.

[55] Gold JI, Shadlen MN. The neural basis of decision making. Annual review of neuroscience. 2007 Jul 1;30(1):535-74.

[56] Ariani G, Pruszynski JA, Diedrichsen J. Motor planning brings human primary somatosensory cortex into action-specific preparatory states. Elife. 2022 Jan 12;11:e69517.